Effect of N doping on the electron emission properties of diamondlike carbon film on a 2-in. Mo field emitter array panel*

Jae Hoon Jung,[a] Byeong Kwon Ju, Hoon Kim,
and Myung Hwan Oh
Electronic Materials and Devices Research Center, KIST, Seoul 130-650, Korea

Suk Jae Chung and Jin Jang
Department of Physics, Kyung Hee University, Seoul 130-701, Korea

(Received 19 August 1997; accepted 26 January 1998)

We have studied the enhancement of field-emission characteristics by hydrogen-free nitrogen-doped diamondlike carbon (DLC) coating on Mo-tip field emitter arrays by a layer-by-layer technique using plasma-enhanced chemical vapor deposition. The Spindt-type molybdenum tip is used as an emission source without a resistive layer on the silicon substrate. The maximum emission current for each pixel was increased from 160 to 1520 μA by a 20 nm N-doped DLC coating. Furthermore, the emission current from DLC-coated field emitter arrays (FEAs) is more stable than that of noncoated FEAs. © *1998 American Vacuum Society.* [S0734-211X(98)07302-8]

I. INTRODUCTION

The Spindt-type cathode is commonly used to achieve uniform field emitter arrays (FEAs).[1] However, the technology is not well optimized for field-emission display (FED) fabrication based on electron emission stability. The interest for diamondlike carbon (DLC) as an emission material originates from its unique emission properties of low threshold field as well as stable operation. In addition, high current could be obtained because of its high thermal conductivity. The microprotuberances on the Mo tip at the critical temperature would be destroyed, resulting in a decrease in the effective emitting area, and thus, degradation in field-emission performance. Degradation can be alleviated by coating the Mo emitter with a material having a high thermal conductivity or designing the tip with more heat sinks. Therefore, we selected DLC thin films with a high thermal conductivity for the coating on Mo tips.

Diamond films possessing negative electron affinity[2] have great potential in their application as electron emitters in vacuum microelectronics such as FEAs and have attracted extensive studies. The field strength required for electron field emission has been reduced to less than 3×10^4 V/cm, which is substantially lower than the field strength used in the conventional metal FEAs, typically, higher than 1×10^6 V/cm.[3]

There has been much interest in the development of diamond and DLC-based electronic devices for high-speed, high-temperature, and high-power applications. For these devices, it is necessary to dope diamond and DLC *n* type. However, *n*-type doping of DLC film has been thought to be very difficult due to the high density of states in the gap near the Fermi level and autocompensation effect, in which doping is accompanied by an increased defect density.[4] In DLC, relatively low E_d (defect creation energy) of π-like defects (lower than 0.4 eV) results in greater compensation and a much lower doping efficiency.

DLC films can be deposited by various growth methods such as plasma-enhanced chemical vapor deposition (PECVD) and filtered vacuum arc deposition. The DLC films deposited by a layer-by-layer technique[5] have no hydrogen inside when the CF_4 plasma exposure time is higher than 120 s and each layer thickness is 5 nm, so that we fixed the CF_4 plasma exposure time at 120 s. In previous work, we have reported on the electron emission characteristics of hydrogen-free DLC-coated Mo FEAs using conventional PECVD.[6,7]

The *n*-type doping of a tetrahedral amorphous carbon (ta-C) with phosphorus and nitrogen has been reported.[8] Nitrogen is the best atom for *n*-type doping because it is a shallow donor compared with phosphorus.[9] In this article, we report on the electron emission behavior of gas-phase, nitrogen-doped hydrogen-free DLC-coated Mo FEAs using conventional PECVD.

In the present work, we have fabricated a 2-in. Mo-tip FEA panel and coated N gas-phase doped DLC on Mo FEAs by a layer-by-layer technique using PECVD, and compared its electron emission behavior with noncoated Mo FEAs as well as report the current status of FEAs development with a reliability test.

II. EXPERIMENT

A 2-in. Mo-tip FEA panel was fabricated by electron-beam evaporation of Mo onto a Si wafer with 1.5 μm diam holes spaced on 7 μm centers. This pattern resulted from the sequential processes of Cr deposition and Al coating, followed by forming *n* well and patterning the gate layers. During DLC deposition, the substrate temperature was fixed at room temperature under a pressure of 20 mTorr. A thin DLC layer about 5 nm thick was deposited and then the surface was exposed to CF_4 plasma for 120 s because CF_4 plasma can remove the weak bond, predominantly $C-H_n$ bonds and

*No proof corrections received from author prior to publication.
[a]Electronic mail: jhjung@kistmail.kist.re.kr

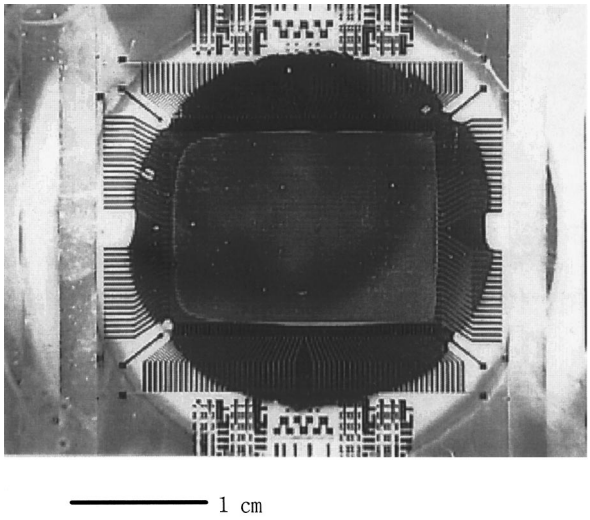

FIG. 1. Completed DLC-coated 2-in. diagonal FEA panel.

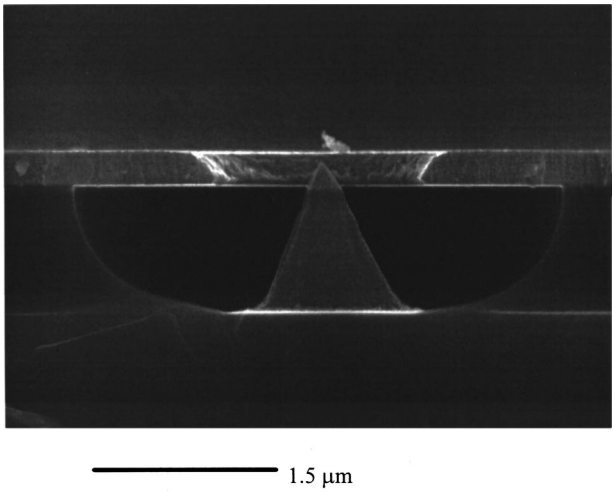

FIG. 2. Cross-sectional view of a DLC-coated Mo field emitter.

graphite C–C bonds.[10] The repeated deposition and CF_4 plasma exposure gave rise to a 20 nm thick DLC film. A conventional PECVD system was used to deposit the DLC layer by a $CH_4N_2/H_2/He$ mixture to produce CF_4 plasma.

A phosphor anode (ZnO:Zn thick film on ITO glass) plate was placed at 1 mm above the gate and was biased to +300 V. Both the anode and gate currents were measured as a function of gate-to-cathode bias voltage in a vacuum of 1×10^{-8} Torr using a Kiethyley SMU 237 meter. During testing, the device was in a common emitter configuration with the emitter grounded, and both the anode and gate being positive potentials, to turn the device on.

III. RESULTS AND DISCUSSION

Figure 1 is a photograph of the completed 2-in. diagonal FEA panel. The FEA panel is 56 mm×65 mm in size on a 4-in. Si wafer. The pixel is composed of 4×6 subpixels and each subpixel consists of 7×7 field emitters. The cathode plate has a Mo microtips of 9 million on the 2-in. FEA panel.

The morphologies of the N-doped DLC-coated Mo FEAs observed by scanning electron microscopy shown in Fig. 2 reveal that the emitter is, typically, 1.4 μm high and the gate aperture is 1.5 μm wide. The thicknesses of the thermal SiO_2 and DLC layer were 1.2 μm and 20 nm, respectively.

Figure 3 shows a comparison of the emission current–voltage characteristics between the N-doped DLC, layer-by-layer DLC-coated Mo FEAs, and noncoated Mo FEAs composed of 1176 emitters for one pixel. The turn-on voltage decreases from 55 to 30 V by the layer-by-layer DLC coating, and to 27 V by the N-doped DLC coating. In addition to the decrease in turn-on voltage, the maximum anode current is also increased from 160 to 1520 μA. This indicates that the operating voltage can be remarkably decreased by adopting the DLC layer on Mo FEAs. And, the increase of emission current is related to the shift of the of the Fermi level by nitrogen doping on DLC films. The gate current is less than 1.2% of the anode current for the N-doped DLC-coated Mo FEAs, but 6.25% for pure Mo FEAs at the anode current. The electric field seems to be concentrated at the tip-top of the Mo FEAs by a thin DLC coating, resulting in increasing the emission current and decreasing the leakage (gate) current.

Figure 4 shows a comparison of Fowler–Nordheim (F–N) plots between the N-doped DLC, layer-by-layer DLC-coated Mo FEAs, and noncoated Mo FEAs. The field-enhancement factor (β) for the emitter was first obtained by comparing the ϕ value calculated from the slope of the F–N plots[1] of the Mo FEAs with the work function reported for Mo metal (4.5

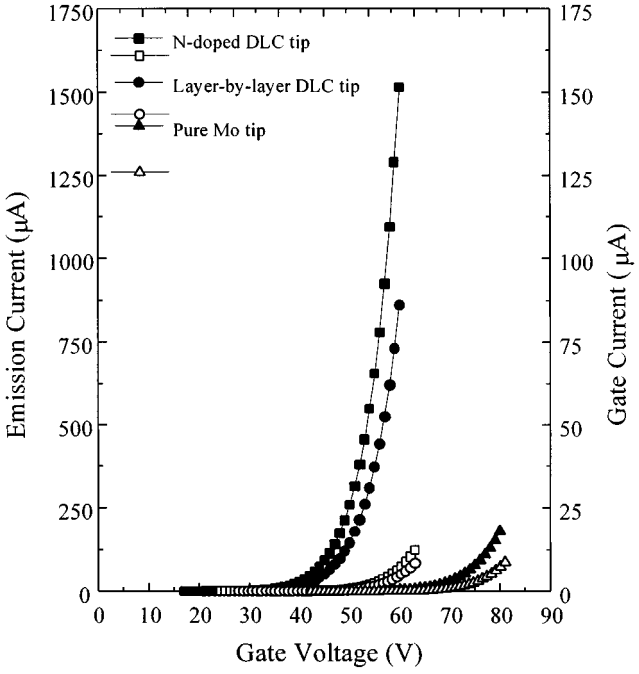

FIG. 3. Comparison of the $I-V$ characteristics of the N-doped DLC, layer-by-layer DLC-coated Mo FEAs and noncoated Mo FEAs.

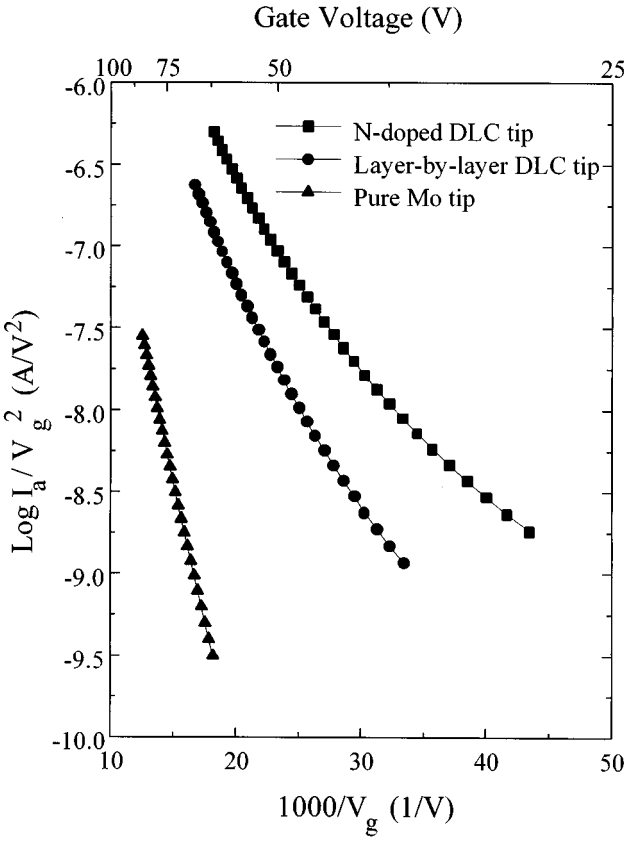

FIG. 4. Fowler–Nordheim plots of the N-doped DLC, layer-by-layer DLC-coated Mo FEAs, and noncoated Mo FEAs.

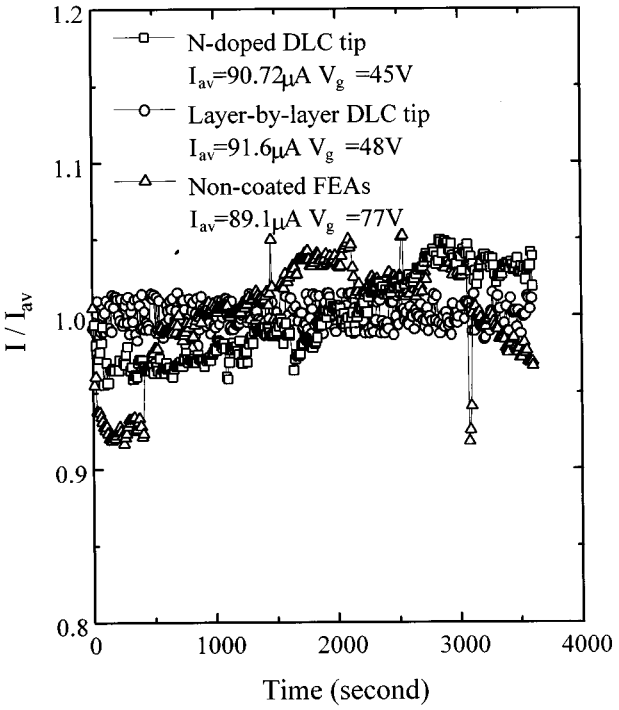

FIG. 5. Emission current fluctuations of the N-doped DLC, layer-by-layer DLC-coated Mo FEAs, and noncoated Mo FEAs.

eV). The effective ϕ values calculated for the layer-by-layer DLC and N-doped DLC-coated FEAs are 2.1 and 1.9 eV, respectively, which are much less than that of the Mo work function, so that the work function seems to be lowered by the DLC coating. We should calculate the effective work functions of the Mo tip and DLC-coated Mo tip by comparison of the slope of each case in the Fowler–Nordheim plot in the following equation:

$$\phi_{\mathrm{Mo}}/\phi_{\mathrm{DLC}}=(S_{\mathrm{Mo}}/S_{\mathrm{DLC}})^{2/3},$$

where ϕ and S are the work function of emitting materials and the slope in the F–N plot, respectively. This calculated effective work function of the DLC-coated Mo tip is not accurate. But we try to show briefly the comparison of the work function of each tip by rough calculation in this study.

Table I depicts the simulation data of the maximum electric field on tip-top with various tip radius and anode voltage at 100 V of fixed gate voltage. It is confirmed that the maximum electric field on tip-top is decreased with increasing tip radius as shown in Table I. The tip radius of the pure Mo tip is 400 Å and that of the DLC-coated Mo tip is 600 Å in this case. It is known that the emission current is decreased with increasing tip radius. However, in spite of the increasing tip radius by the DLC coating, the emission current of our devices is increased because the electron emission performance of DLC is better than other emitting materials (Mo, Si, etc.).

Figure 5 shows the emission current fluctuations for N-doped DLC, layer-by-layer DLC-coated Mo FEAs and noncoated Mo FEAs with fixed gate voltages giving almost the same current level. The overall current fluctuation is very small for the DLC-coated arrays, but the current tends to decrease with time for the noncoated Mo FEAs. However, there is some fluctuation of current for the DLC-coated arrays even though its average current is almost constant with time. The current variation of the N-doped DLC, layer-by-layer DLC-coated Mo FEAs and noncoated Mo FEAs is 2.1%, 1.9%, and 8.9%, respectively. Excellent long-term current stability and reproducibility in the range of a few 100 μA over a period of several hours was obtained for N-doped DLC and layer-by-layer DLC-coated Mo FEAs. The im-

TABLE I. Maximum electric field on tip-top with various tip radius and anode voltage.

Tip radius \ Anode voltage	300 V	500 V	1000 V
400 Å	2.227×10^9 V/m	2.229×10^9 V/m	2.234×10^9 V/m
500 Å	1.758×10^9 V/m	1.761×10^9 V/m	1.774×10^9 V/m
600 Å	1.529×10^9 V/m	1.531×10^9 V/m	1.538×10^9 V/m

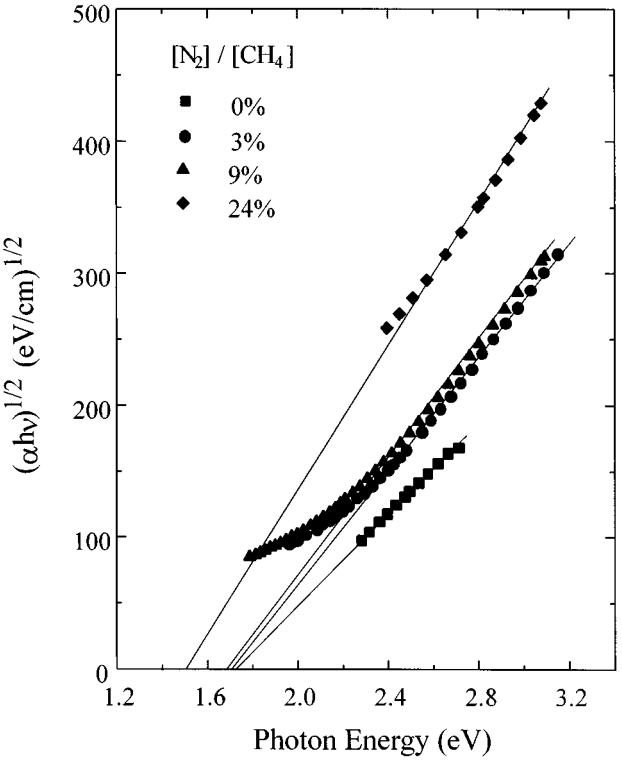

FIG. 6. Tauc' plot of nitrogen gas-phase doped DLC films.

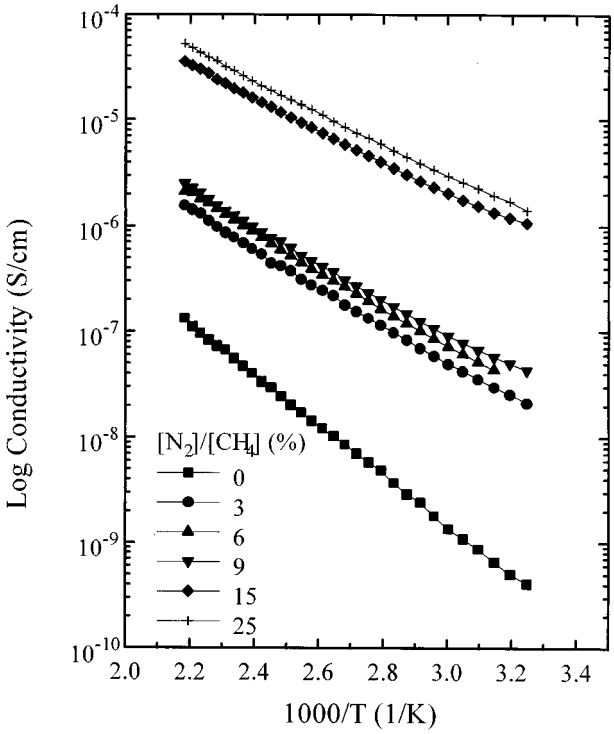

FIG. 7. Temperature-dependent conductivities of the DLC films doped with various $[N_2]/[CH_4]$ ratios.

proved stability by DLC coating appears to be due to its material properties. The structure of DLC films on the microfabricated tip is changed by resistive heating, resulting in the degradation of electron emission,[3] and electron emission instability has been seen on diamond and diamond-coated microtips.[11] However, the origin of the instability of the electron emission current is not clear. The emission current fluctuation seems to be related to the incorporated hydrogen in DLC films deposited by the conventional PECVD system. The bonding energy of $C-H_n$ is lower than that of the C–C bond, resulting in easy bond breaking and rebonding. In conventional DLC, this weak bond breaking and rebonding of the atoms could be repeated because of the high hydrogen content. Therefore, it is expected that our hydrogen-free DLC film has stable electron emission.

The DLC films deposited by conventional PECVD have instability during operation because of its high hydrogen content, but our DLC films, having no hydrogen inside, are very stable under long-time operation.

We also studied on the characteristics of hydrogen-free nitrogen-doped DLC films in order to investigate the role of electron emission of Mo FEAs by DLC coating.

Figure 6 shows a Tauc' plot of the N-doped DLC film with various nitrogen gas. The optical band gap (E_g), obtained from the slope of the Tauc' plot, decreased by nitrogen doping. The decrease in the slope is related to the plasma and/or radiation damage, which causes the conversion of sp^3 C to sp^2 C. Note that the conversion of sp^3 to sp^2 reduces the band gap of DLC.

The increase of emission current is related to the shift of the Fermi level and subsequent increase of the carrier density in the DLC film. Figure 7 shows the temperature-dependent conductivities of DLC films with various nitrogen gases. The conductivity increases from 4.1×10^{-10} to 1.4×10^{-6} S/cm when the $[N_2]/[CH_4]$ ratio changes from 0% to 25%, because the Fermi level is shifted toward the conduction band by n-type doping. When the $[N_2]/[CH_4]$ ratio is above 15%, the conductivity increases steadily because all films show n-type behavior. The conductivity increases, and thus, the activation energy decreases from 0.46 to 0.30 eV with the increasing $[N_2]/[CH_4]$ ratio when the $[N_2]/[CH_4]$ ratio is less than 15%, but after that the conductivity increases steadily by the continuous shift of the Fermi level toward the conduction band, caused by accumulated nitrogen atoms in the DLC films.

The temperature dependence of conductivity was measured, and the prefactor of conductivity and conductivity activation energy were obtained. The dc electrical conductivity of the semiconductor in the extended state is described as[12]

$$\sigma=\int\{N(E)\mu(E)f(E)[1-f(E)]\}=eN(E_c)kT\mu_c \times\exp\{-(E_c-E_F)/kT\}=\sigma_0\exp(-E_a/kT),$$

where μ_c is an average mobility at E_c, E_a is $E_c(0)-E_F(\tau)+(dE_F/d\tau)$ and $\sigma_0=eN(E_c)kT\mu_c$, which is called the minimum metallic conductivity. The σ_0 is related to the statistical shift of the Fermi level:

$$\sigma_0=\sigma_{00}\exp[-(dE_c/d\tau)+(dE_F/d\tau)] =\sigma_{00}\exp(r_c)\exp(dE_F/d\tau),$$

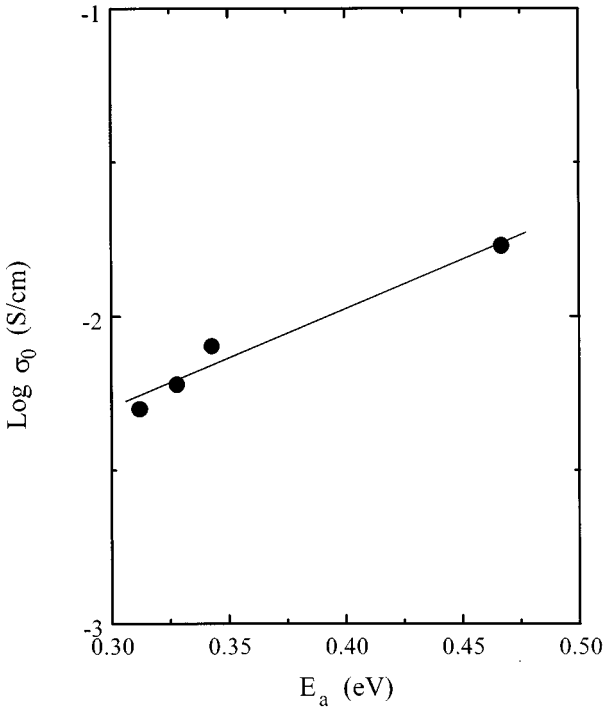

FIG. 8. Meyer–Nedel relation between the prefactor of conductivity and conductivity activation energy of nitrogen-doped DLC films.

because $E_c(\tau)=E_c(0)-r_c\tau$.

The Meyer–Nedel relation is described as

$$\sigma_0=\sigma_{00}\exp(AE_a)=\sigma_{00}\exp(r_c)\exp(dE_F/d\tau)$$
$$=\sigma_{00}\exp(AE_a).$$

Figure 8 shows the Meyer–Nedel relation between the prefactor of conductivity and conductivity activation energy for a series of nitrogen-doped DLC films. The Meyer–Nedel relation $\sigma_0=\sigma_{00}\exp(AE_a)$ is well satisfied with $A=3.63\ \mathrm{eV}^{-1}$ and $\sigma_{00}=2.3\times10^{-4}$ S/cm. The A is lower than that ($\sim20\ \mathrm{eV}^{-1}$) for hydrogenated amorphous silicon.[13] And, the film has a much smaller σ_{00} value, which is related to the smaller carrier mobility of DLC compared to an *a*-Si:H.

We have demonstrated that N-doped DLC and layer-by-layer DLC-coated Mo FEAs are very stable under operation when hydrogen-free DLC film is deposited by a layer-by-layer deposition technique. It is important to use hydrogen-free and N-doped DLC instead of conventional DLC. The PECVD used in the present work can be applied to deposit large-area and uniform films with low cost, so that our DLC could be applied to the mass production of FEDs.

IV. CONCLUSION

The electron emission characteristics of nitrogen-doped DLC, layer-by-layer DLC-coated Mo FEAs, and conventional Mo FEAs have been studied in order to develop a stable 2-in. Mo FEA panel. The DLC layer in the present work was prepared by a layer-by-layer deposition technique and *n*-type doping. The electron emission from the FEAs is much improved by a thin layer of DLC coating on the Mo FEAs. Moreover, the stability is much improved by adopting the hydrogen-free nitrogen-doped DLC.

[1]C. A. Spindt, I. Bodie, L. Humphrey, and E. R. Westerberg, J. Appl. Phys. **47**, 5248 (1976).
[2]F. J. Himpsel, J. A. Knapp, and J. A. Van Vechten, Phys. Rev. B **20**, 624 (1979).
[3]F. Y. Chuang, C. Y. Sun, H. F. Cheng, C. M. Huang, and I. N. Lin, Appl. Phys. Lett. **68**, 1666 (1996).
[4]J. Robertson, Phys. Rev. B **33**, 4399 (1986).
[5]K. C. Park, J. H. Moon, J. Jang, and M. H. Oh, Appl. Phys. Lett. **68**, 3594 (1996).
[6]J. H. Jung, B. K. Ju, Y. H. Lee, J. Jang, and M. H. Oh, IEEE Electron Device Lett. **18**, 197 (1997).
[7]J. H. Jung, B. K. Ju, Y. H. Lee, M. H. Oh, and J. Jang, Tech. Digest Int. Electron Devices Meet. 293 (1996).
[8]D. I. Jones and A. D. Steward, Philos. Mag. B **46**, 423 (1982).
[9]V. S. Veersamy, J. Yuan, G. A. J. Ammaratunga, W. I. Milne, K. W. R. Gilkes, M. Weiler, and L. M. Brown, Phys. Rev. B **48**, 954 (1993).
[10]Y. Shimada, N. Mutsukura, and Y. Machi, J. Appl. Phys. **71**, 4019 (1992).
[11]V. V. Zirnov, A. B. Voronin, E. I. Givargizov, and A. L. Meshcheryakova, Tech. Digest of IVMC'95, p. 340, 1995.
[12]J. I. Pankove, Semiconductor and Semimetals, Vol. 21, Part C, Chap. 8, 1984.
[13]H. Fritzsche, Sol. Energy Mater. **3**, 447 (1988).